Applied Surface Science 255 (2009) 5245–5247

Contents lists available at ScienceDirect

Applied Surface Science

journal homepage: www.elsevier.com/locate/apsusc

Thin films of semiconducting lithium ferrite produced by pulsed laser deposition

R.D. Gunning *, Karsten Rode, Sumesh R.G. Sofin, M. Venkatesan, J.M.D. Coey, Igor V. Shvets, James G. Lunney

CRANN and School of Physics, Trinity College Dublin, Ireland

ARTICLE INFO

Article history:
Available online 6 November 2008

Keywords:
Ferromagnetic
Semiconducting
Lithium ferrite
Mossbauer
Hall effect

ABSTRACT

Thin films of lithium ferrite ($Li_{0.5}Fe_{2.5}O_4$) have been deposited on (0 0 1) Al_2O_3 by pulsed laser deposition, with substrate deposition temperatures ranging between 500 and 800 °C, and oxygen pressures between 1×10^{-1} and 4×10^{-7} mbar. X-ray diffraction shows that films grow with a (1 1 1) orientation. Conversion electron Mössbauer spectra for the high-pressure films show a single sextet with a hyperfine field of 49 T, while the low-pressure films show two sextets with hyperfine fields of 47 and 49 T. The spectra also reveal paramagnetic ferric iron in both types of films. Magnetization measurements of the films show a saturation magnetization of between 1.7 and 3.1 μ_B per formula unit and a coercivity of between 10 and 44 mT. The films prepared under the lower oxygen pressures are semiconducting with resistivities of 2×10^{-2} to 8×10^{-2} Ω cm. They exhibit an anomalous Hall effect with p-type conduction at 175 K.

1. Introduction

The emergence of spintronics, the integration of the electron's spin into conventional electronics, has created the demand for a new and elusive class of material – the ferromagnetic semiconductor [1]. To date, the search for this class of material has been focussed on inducing ferromagnetism in a host semiconductor matrix, such as GaN [2], ZnO [3] or SnO_2 [4] by substituting magnetic ions such as Mn, Fe or Co. There have been suggestions [5] that a semiconducting material can become ferromagnetic due to crystal imperfections. All these approaches centre on inducing ferromagnetism in a semiconductor by magnetic substitution. There is, however, another possibility – inducing semiconductivity in an insulating ferromagnet by electronic doping.

Lithium ferrite is a stable, insulating ferrimagnet [6], that has applications as a microwave material [7]. It is a close relative of magnetite, which can be represented as $[Fe^{3+}]\{Fe^{3+}Fe^{2+}\}O_4$, where the square bracket represents the tetrahedral site and the curly bracket represents the octahedral site. For magnetite, 8 of the 16 Fe^{3+} ions in the unit cell occupy the tetrahedral sites, whereas the other 8, together with the 8 Fe^{2+}, ions occupy the octahedral sites. Lithium is monovalent, so for $Li_{0.5}Fe_{2.5}O_4$, all the Fe must be in the 3+ valence state, giving $[Fe^{3+}]\{Fe^{3+}{}_{1.5}Li^{+}{}_{0.5}\}O_4$, assuming the inverse spinel structure. Any Li deficiency in the lattice would give rise to Fe^{2+}. Given the antiparallel coupling of tetrahedral and octahedral sites, the formula implies a magnetic moment of 2.5 μ_B per formula unit. It is expected that a material with less than the stoichiometric Li content will have a mixture of Fe^{2+} and Fe^{3+} on octahedral sites and may exhibit semiconducting behaviour.

2. Experimental

Ceramic targets were prepared by the mechanical mixing of the correct amounts of $LiCO_3$ and Fe_2O_3, and then pressed into circular pellets. The pellets were then heated slowly by 1 °C min^{-1} to 600 °C, and left at this temperature for 1 h. The targets were then sintered at 1000 °C for 12 h and left to cool. The thin films were prepared by the ablation of these pellets with a Lambda Physik Compex Pro KrF Excimer laser operating at λ = 248 nm. The fluence of the beam was 2 J cm^{-2}, with a pulse frequency of 10 Hz. The films were deposited onto single crystal c-cut (0 0 1) Al_2O_3 substrates at temperatures ranging between 500 and 800 °C. The base pressure attained in the chamber was 1×10^{-7} mbar. The substrates were cleaned by heating to 800 °C and flushing with 3×10^{-1} mbar of O_2 prior to deposition. The films were deposited in a pressure of O_2 ranging between 4×10^{-7} and 1×10^{-1} mbar. Reflection high energy electron diffraction was used to monitor crystal growth in situ, using a KSpace RHEED. Carrier concentration and carrier type were measured by the observation of the Hall effect in the thin films. The films were patterned into Hall bars with eight contacts and the Hall voltage and magneto-resistance were measured simultaneously. A field of up to 5 T was applied using a Quantum design PPMS, and the variations in Hall voltage with this field measured.

* Corresponding author.
E-mail address: gunninr@tcd.ie (R.D. Gunning).

0169-4332/$ – see front matter © 2008 Elsevier B.V. All rights reserved.
doi:10.1016/j.apsusc.2008.10.105

X-ray diffraction was performed on both the target pellets and the thin films to determine the crystal structure and orientation using a PANalytic X'Pert Pro with Cu Kα radiation (λ = 0.154056 nm). Film thicknesses were measured using small angle X-ray reflectivity.

Magnetization measurements were carried out using a Quantum Design superconducting quantum interference device (SQUID) and an alternating gradient force magnetometer (AGFM).

3. Results

The diffractograms of the ceramic targets confirmed the presence of the $Li_{0.5}Fe_{2.5}O_4$ phase. No secondary phases were detected in the targets, but traces of a secondary phase, $Li_2Fe_3O_4$, were found in the targets after ablation. The diffractograms of all films deposited on c-cut sapphire show films with an inverse spinel structure, with a (1 1 1) axis orientation (Fig. 1). For the films grown at higher oxygen pressures (1×10^{-1} mbar), a secondary phase of hematite is observed.

The films deposited at the lower oxygen pressures (4×10^{-6} mbar) exhibit a saturation magnetization, σ, of 40 to 70 A m^2 kg^{-1} depending on deposition temperature (Fig. 2). There is no clear relationship between the deposition temperature and σ. The films also exhibit a small coercive field of around 30 mT.

^{57}Fe Mössbauer spectroscopy with a ^{57}Co/Rh source was performed to characterize the iron in the samples (Fig. 3). A transmission Mössbauer set-up was used on powder scraped from the ceramic target while a conversion electron Mössbauer spectroscopy (CEMS) was used for the thin films. The spectra were fitted using the standard least-squares method.

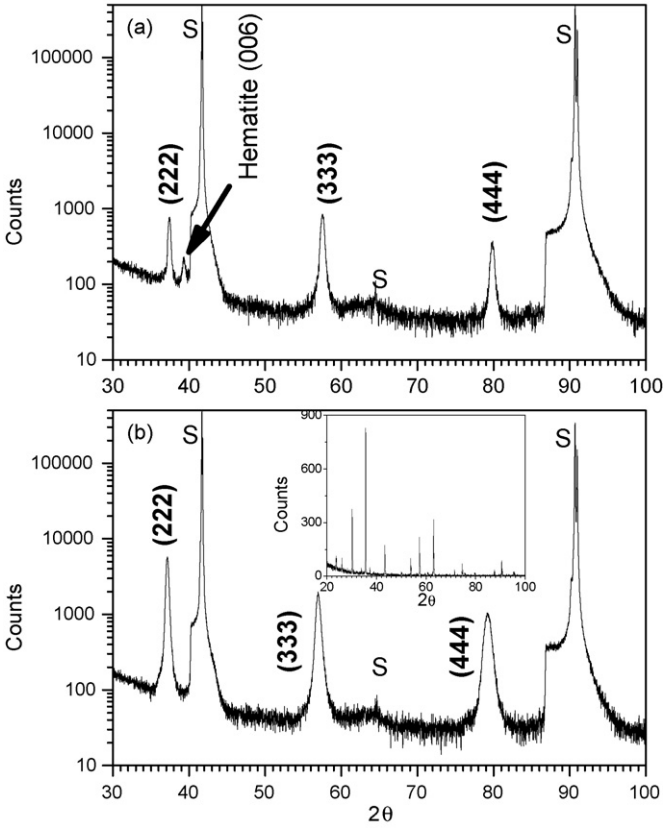

Fig. 1. X-ray diffraction pattern of high-pressure (a) and low-pressure (b) films of $Li_{0.5}Fe_{2.5}O_4$ on c-cut sapphire. The films exhibit (1 1 1) texture. Substrate peaks are marked with an 'S'. *Inset*: X-ray diffraction pattern of the ceramic target.

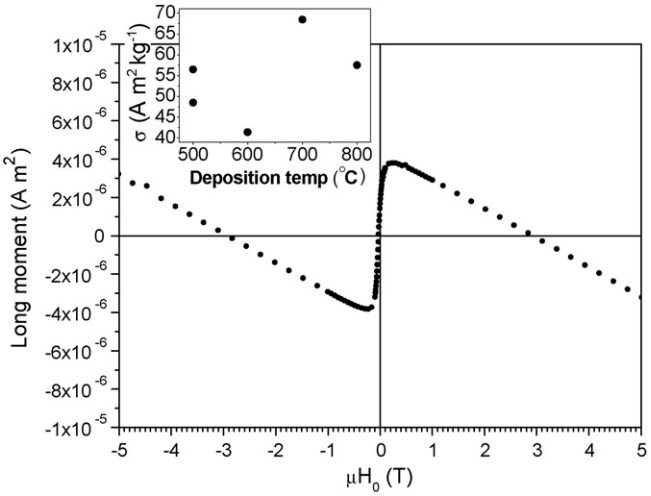

Fig. 2. Room temperature magnetization curve for a lithium ferrite film deposited at 4×10^{-6} mbar. The data are not corrected for the diamagnetism of the substrate.

The transmission Mössbauer spectra showed a single sextet with and isomer shift of 0.42 mm s^{-1} relative to α-Fe and a hyperfine field of 50.3 T. For the thin films deposited at higher oxygen pressure, the spectra were fitted with a sextet, with an isomer shift of 0.43 mm s^{-1} and a slightly lower hyperfine field, B_{HF} = 49.3 T. The films deposited at a lower pressure resemble the spectra of magnetite. They were fitted with two sextets, with isomer shifts of 0.36 and 0.88 mm s^{-1}, and B_{HF} of 48.7 and 46.7 T, respectively. The intensity ratio is 60:40. The lower isomer shift is due to Fe^{3+}, while the higher isomer shift is due to a mixed valence

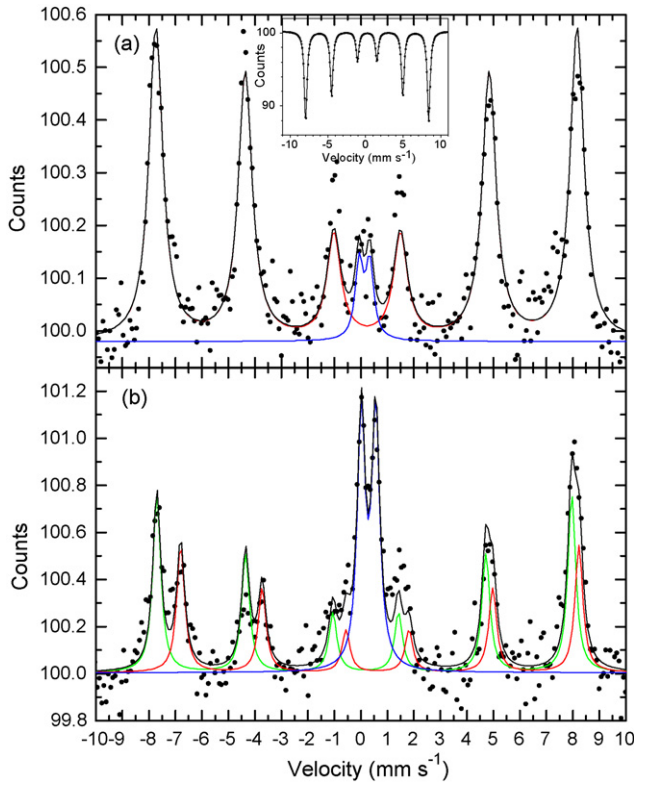

Fig. 3. Conversion-electron Mössbauer spectra of films deposited at (a) 1×10^{-1} mbar and (b) 4×10^{-6} mbar. *Inset*: Transmission Mössbauer spectra of ceramic target.

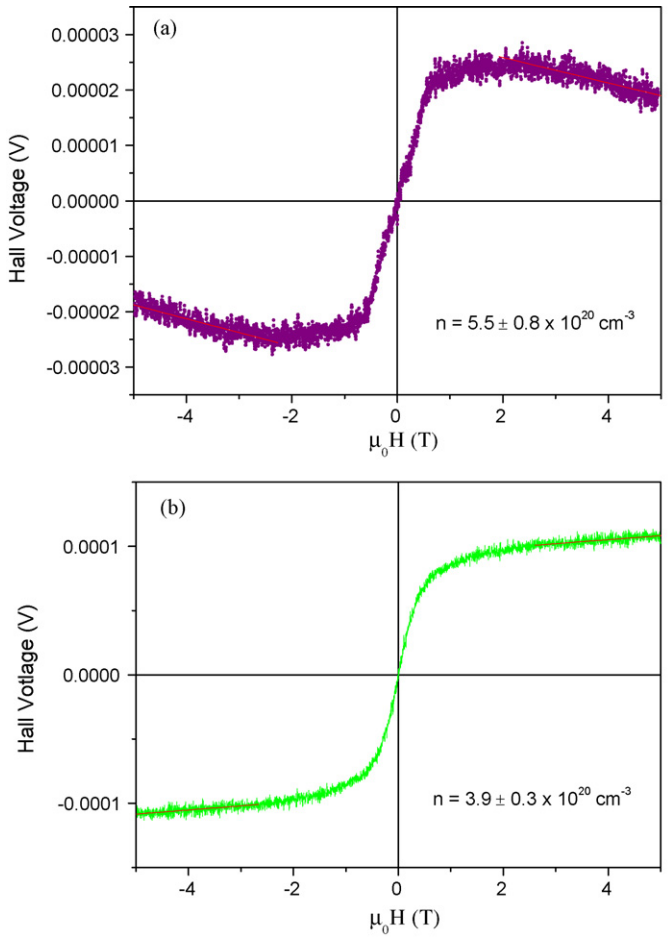

Fig. 4. Hall effect measurement at (a) 175 K and (b) 300 K for a lithium ferrite film deposited at 4×10^{-6} mbar.

of Fe^{2+} and Fe^{3+} in a ratio of 2:3. Hence, we estimate that 24% of the magnetically ordered iron is Fe^{2+}. The Mössbauer spectra of both the high- and low-pressure films also showed a paramagnetic doublet with isomer shifts of 0.34 mm s^{-1} for the high-pressure films and 0.49 mm s^{-1} for the low-pressure films. The doublet accounted for only 5% of the total iron in the high-pressure films, but was more significant in the low-pressure films, accounting for 23% of the total iron in the film. Assuming this iron here is also mixed valence in the same ratio, the expected isomer shift would be 0.55 mm s^{-1}.

The spectra of the films deposited at the higher oxygen pressures are similar to the spectra of the ceramic targets, which are true $Li_{0.5}Fe_{2.5}O_4$ according to the XRD. The spectra of the films deposited at the lower pressures resemble that of magnetite, which suggests that they are Li-deficient. The large paramagnetic doublet in the low-pressure films suggests that the iron is superparamagnetic as no major secondary phase was seen by XRD (Fig. 1).

The Hall measurements are shown in Fig. 4. Data at 300 and 175 K for a typical low-pressure film show a large anomalous Hall effect. The Hall resistance in a ferromagnet usually has two contributions; the normal Hall effect which is proportional to the applied field, and the anomalous Hall effect which is proportional to the magnetization:

$$\frac{V_H}{I} = \left(\frac{R_H}{t}\right)\mu_0 H + \left(\frac{R_S}{t}\right)\mu_0 M$$

where t is the film thickness and H and M are assumed to be parallel and perpendicular to both the electrical current and the sample surface. The measurements taken at 175 K give a carrier concentration $n = 5.5 \pm 0.8 \times 10^{20}$ cm^{-3} and a mobility of $2.2 \pm 0.3 \times 10^{-2}$ cm^2 V^{-1} s^{-1} (Fig. 4). The carrier sign was positive at 175 K. Below 175 K, the resistivity of the sample was too large for meaningful measurements to be obtained. It is hazardous to estimate the Hall resistivity from the room temperature data, where the magnetization is probably unsaturated due to superparamagnetic contributions. The high-pressure film is insulating at room temperature.

4. Discussion

From examination of the X-ray diffractograms and the Mössbauer spectra, we can see that deposition at the two different oxygen pressures results in two distinct materials. At 10^{-1} mbar of oxygen (high pressure) a stoichiometric, insulating lithium ferrite phase is obtained. This is confirmed by the (1 1 1) oriented peaks observed in the X-ray diffractograms and a single sextet in the Mössbauer spectra. Moreover, the Mössbauer spectrum matches that of the polycrystalline target which is confirmed to be lithium ferrite by X-ray diffraction.

The films deposited at the lower pressures (10^{-6} mbar) contain ferrous iron on octahedral sites, and show a spectrum which is characteristic of a mixed valence state, similar to that found in magnetite (Fig. 3). The lithium content of the film is not expected to depend on oxygen pressure, but the films deposited at the lower oxygen pressures are expected to be oxygen deficient $Li_{0.5}Fe_{2.5}O_{4-\delta}$. From the Fe^{2+}/Fe^{3+} ratio, 24/76, deduced in the previous section, we infer $\delta = 0.30$. If instead we use the isomer shift to deduce the ferrous fraction of the paramagnetic absorption we find $\delta = 0.28$.

Both materials are ferromagnetic. The observed moment for the lithium ferrite films ranged between of 1.8 and 3.0μ_B per formula unit, which may be compared with 2.5μ_B calculated for the stoichoimetric material and 1.9μ_B expected from the formula of the non-stoichiometric film. Of these two different sample types, only the off-stoichiometric material is conducting. Unlike magnetite, the material is a p-type semiconductor at 175 K.

5. Conclusions

We have successfully grown (1 1 1) orientated lithium ferrite on (0 0 1) sapphire by pulsed laser ablation. The oxygen deficient material is a p-type magnetic semiconductor with a high Curie temperature. The mobility is low but there may be potential applications in oxide spin devices.

References

[1] S.A. Wolf, D.D. Awschalom, R.A. Buhrman, J.M. Daughton, S. von Molnar, M.L. Roukes, A.Y. Chtchelkanova, D.M. Treger, Science 294 (2001) 1488–1495.
[2] S. Sonoda, S. Shimizu, T. Sasaki, Y. Yamamoto, H. Hori, Journal of Crystal Growth 237–239 (2002) 1358–1362.
[3] M. Venkatesan, C.B. Fitzgerald, J.G. Lunney, J.M.D. Coey, Physical Review Letters 93 (2004) 177206–177214.
[4] C.B. Fitzgerald, M. Venkatesan, L.S. Dorneles, R. Gunning, P. Stamenov, J.M.D. Coey, P.A. Stampe, R.J. Kennedy, E.C. Moreira, U.S. Sias, Physical Review B (Condensed Matter and Materials Physics) 74 (2006) 115307–115310.
[5] C.D. Pemmaraju, S. Sanvito, Physical Review Letters 94 (2005) 217205–217214.
[6] H.J. Masterson, J.G. Lunney, D. Ravinder, J.M.D. Coey, Journal of Magnetism and Magnetic Materials 140–144 (1995) 2081–2082.
[7] W.G. Nilsen, R.L. Comstock, J.P. Remeika, Journal of Applied Physics 37 (1966) 1224–1225.